Textural Characteristics and Energetic Parameters of Activated Carbon Monoliths: Experiments and Monte Carlo Simulations†

Diana P. Vargas[1], J.C. Alexandre de Oliveira[3], Liliana Giraldo[1], Juan Carlos Moreno-Piraján[2*], R.H. López[3] and G. Zgrablich[3] *(1) Department of Chemistry, Faculty of Science, National University of Colombia, Av. Carrera 30 No. 45-03 Bogotá, Colombia. (2) Porous Solids and Calorimetry Research Group, Department of Chemistry, Faculty of Science, University of the Andes, Carrera 1a, No.18a-10, Bogotá, Colombia. (3) INFAP-CONICET, Department of Physics, University National de San Luis 950, CP: 5700, San Luis, Argentina.*

(Received 29 March 2011; accepted 14 July 2011)

ABSTRACT: Disc-type activated carbon monoliths were prepared through chemical activation of coconut shell and African palm pits with phosphoric acid at different concentrations, without using any binder. The structures thereby produced were studied experimentally by nitrogen adsorption at 77 K, carbon dioxide adsorption at 273 K and immersion calorimetry in benzene. The experimental data allowed the textural and energetic characterization of the microporous solids to be obtained, viz. BET areas between 752 and 1711 m^2/g, micropore volumes between 0.32 and 0.61 cm^3/g, ultramicropore volumes between 0.11 and 0.24 cm^3/g and immersion enthalpy values between 95.85 and 147.7 J/g. Grand Canonical Monte Carlo (GCMC) simulations were used to analyze the experimental results, providing an interpretation of, as well as a more detailed characterization, of the textural properties, such as the determination of the pore-size distribution (PSD) of each material.

1. INTRODUCTION

The term "activated carbon" applies to a group of microporous carbons prepared by reaction of a carbonized material with an oxidizing gas or by the carbonization of lignocellulosic materials impregnated with chemical dehydrating agents. The activated carbons are disordered solids consisting primarily of carbon, with a high degree of porosity and high internal surface, which are of significance in adsorption and catalysis. The porous structure of these materials consists of small graphitic sheets stacked as imperfect micro-crystallites, interlocking to create a three-dimensional network whose empty space constitutes the porosity (Bansal and Goyal 2005; Budinova *et al*. 2006).

This adsorbent can be produced in the form of fibres, powders, granules, fabrics and monolithic structures, amongst others (Yates *et al*. 2000). Because of their characteristics, the so-called activated carbon monoliths (ACMs) are at present being used as effective adsorbents and catalyst supports for environmental decontamination. The monoliths may be produced in different forms, such as compact discs and honeycomb monoliths, the latter being unitary structures traversed lengthwise by parallel channels. These represent a new concept in the design of catalysts supports

† Published in the Festschrift of the journal dedicated to Professor Giorgio Zgrablich on the occasion of his 70th birthday and to celebrate his 50 years as a faculty member at the National University of San Luis in Argentina.

* Author to whom all correspondence should be addressed. E-mail: jumoreno@uniandes.edu.co.

and absorbents, featuring low values of load loss in the passage of gases thereby facilitating their smooth flow, convenient mechanical properties and a large geometric surface per unit weight or volume. They also behave as nearly adiabatic systems and reduce the constraints generated by internal diffusion phenomena (Rodríguez-Reinoso *et al*. 2003; Liu *et al*. 2006).

The physical adsorption of gases, vapours and liquids is one of the most popular techniques used to study the porous texture of solids of all kinds. In the characterization of the porous texture of a solid, the main properties to be determined are the surface area (or specific surface area), the micropore volume and the pore-size distribution (PSD) (Rodríguez-Reinoso and Molina-Sabio 1998; Sing 2004). The adsorption of nitrogen at 77 K and of carbon dioxide at 273 K is normally used for the determination of these properties by measuring the corresponding adsorption isotherms (James 2006; Sing 1989), which are then analyzed via appropriate theoretical models in order to finally obtain the desired information.

In recent years, Monte Carlo simulation methods have been used as a convenient theoretical tool to predict the textural and energetic characteristics of adsorbents such as activated carbons. These methods have the advantage that the results will depend only on the accuracy of the interaction potentials assumed. In the Grand Canonical Monte Carlo (GCMC) simulation, the temperature, volume and chemical potential (which can be directly related to the pressure and the temperature using the bulk gas equation of state) are specified, while the number of particles and associated configurational energy are allowed to fluctuate. Hence, GCMC sampling is capable of yielding directly the amount adsorbed in arbitrary confined spaces as a function of pressure and temperature, and thus presents a convenient tool for modelling adsorption in pores. This simulation method relies on the actual molecular microscopic configurations of the confined fluid using realistic intermolecular interaction potentials and, in principle within statistical errors, provides exact predictions for the potentials used (Gusev and O'Brien 1997).

In the present study, we have used a slit-like geometry for a collection of independent pores distributed according to a PSD (Valladares *et al*. 1998). Such a configuration has normally been employed over a period of several decades, although other models using different geometries have been developed recently (Azevedo *et al*. 2010). These kinds of models require the assumption of a given geometric shape for the pores and the way in which these are interconnected.

The experimental and theoretical methods described above are applied in this work to the study of 10 ACM samples, obtained by carbonization and chemical activation of two precursor materials, i.e. coconut shells and African palm pits. The textural and energetic properties of these materials have been analyzed through measurements of the adsorption isotherms and immersion calorimetry in benzene.

2. EXPERIMENTAL

2.1. Preparation of the monolithic discs

The precursor was impregnated with solutions of phosphoric acid for 2 h at 85 °C, employing 1 g precursor per 2 mℓ of solution, and then dried at 110 ° C for 4 h. The resulting material was then shaped in a uniaxial press at 150 °C. The structures obtained were carbonized in a horizontal furnace at a linear heating rate of 1 °C/min up to a temperature of 500 °C, and then maintained at this temperature for 2 h under a flow of nitrogen at a flow rate of 85 mℓ/min. Finally, the structures were washed with distilled water up to a neutral pH value to remove traces of the chemical agent employed in the impregnation process (Nakagawa *et al*. 2007; Almansa *et al*. 2004).

Different concentrations of H_3PO_4 (24 w/v%, 28 w/v%, 32 w/v%, 36 w/v% and 48 w/v%) were used to prepare a series of monolithic discs. Such discs are identified by the letters MCO (coconut shell) and MCU (African palm pit) followed by a number corresponding to the concentration used for each sample; holding all other conditions constant, the other conditions employed resulted in a degree of impregnation (g/x pg precursor) for the series of 0.30, 0.35, 0.40, 0.45 and 0.60, respectively.

2.2. Textural characterization

All ACM samples were characterized via the physical adsorption of nitrogen at 77 K and carbon dioxide at 273 K using a Quantachrome Autosorb 3-B instrument. The software provided with the apparatus also allowed the calculation of the micropore volume — by applying the Dubinin–Radushkevich equation to the experimental data — and the BET surface area.

2.3. Immersion enthalpy

Benzene, a molecule with an average diameter of 0.37 nm, was used as the solvent for determining the enthalpies of immersion of the ACM samples. Such measurements were made in an electrically calibrated heat conduction Calvet microcalorimeter (Silvestre-Albero *et al*. 2001; Moreno and Giraldo 2000) employing a stainless steel calorimetric cell. Known amounts of the solid samples (ca. 150–200 mg) were weighed into a glass vial, which was then sealed and joined to the calorimeter cell containing 10.0 mℓ of benzene. When the assembly had attained thermal equilibrium, the vial was broken to allow the solid to be wetted by the liquid, with the heat generated being recorded as a function of time.

3. MOLECULAR SIMULATION

The adsorption of N_2 and CO_2 in slit-like micropores was investigated by GCMC simulations because this method allows a direct calculation of the phase equilibrium between a gaseous phase and an adsorbate phase. The implementation of this simulation method is both well-established and well-documented [see, for example, Valladares *et al*. (1998), Nicholson and Parsonage (1982), and Steele (1974)].

The interaction between adsorbate molecules was modelled using the truncated Lennard-Jones potential:

$$U_{gg}(r) = -4\varepsilon_{gg}\left[\left(\frac{\sigma_{gg}}{r}\right)^{6} - \left(\frac{\sigma_{gg}}{r}\right)^{12}\right] \tag{1}$$

where ε_{gg} and σ_{gg} are the energetic and geometrical parameters of the LJ potential and r is the molecular separation. Each wall of the model graphitic slit pore was represented by a series of stacked planes of LJ atoms. The interaction energy between a fluid particle and a single pore wall at a distance z (measured between the centres of the fluid atom and the atoms in the outer layer of the solid) was described by the Steele 10–4–3 potential (Steele 1974):

$$U_{gs-STEELE}(z) = 2\pi\varepsilon_{gs}\rho_C\sigma_{gs}^2\Delta\left\{\frac{2}{5}\left(\frac{\sigma_{gs}}{z}\right)^{10} + \left(\frac{\sigma_{gs}}{z}\right)^{4} - \frac{\sigma_{gs}^4}{3\Delta(z + 0.61\Delta)^3}\right\} \tag{2}$$

TABLE 1. Parameters Used in the LJ Potentials for the GCMC Simulations[a]

Molecule	σ_{gg} (nm)	ε_{gg}/k_B (K)	σ_{gs} (nm)	ε_{gs}/k_B (K)
CO_2	0.3750	236.1	0.3590	81.3
N_2	0.3615	101.6	0.3494	56.3
Carbon	0.3400	28.0	–	–

[a] Boltzmann constant $k_B = 1.380/650424 \times 10^{-23}$ J/K.

where Δ is the separation between the graphite layers (0.335 nm), ρ_C is the number density of carbon atoms per unit volume of graphite (114 nm^{-3}), and ε_{gs} and σ_{gs} are the solid–fluid Lennard-Jones parameters. The cross-LJ parameters were determined using the standard Lorentz–Berthelot combining rules (arithmetic mean for collision diameter and geometric mean for well depth). The values of the parameters included in the interaction potentials [equations (1) and (2)] are listed in Table 1 (Cao and Wu 2005; Vishnyakov and Neimark 2003).

The GCMC method followed the algorithm outlined by Valladares *et al*. (1998). In each attempt of the GCMC simulation, three types of elementary steps with equal probability were performed randomly (Frenkel and Smit 1996; Allen and Tildesley 1987) — displacement, adsorption and desorption. The transition probabilities for each Monte Carlo attempt were given by the usual Metropolis rules. The lateral dimensions of the cell for the slit geometry were taken as L = 10.3 nm and periodic boundary conditions were used in these directions. The cut-off distance, beyond which the potential is neglected, was set at 5σ. Equilibrium was generally achieved after 10^7 MC attempts, after which mean values were taken over the following 10^7 MC attempts for configurations, spaced by 10^3 MC attempts, in order to ensure statistical independence. The molecules were moved, created or deleted randomly in slit-like micropore unit cells

The accessible pore volume may be defined in such a way that the centre of the molecule should be available in the volume space where the solid–fluid potential is negative. Thus, if z_0 is the distance at which the solid–fluid potential is zero, the accessible width for the adsorbate molecule may be taken as:

$$H' = H_{cc} - 2z_0 + \sigma_{gg} \tag{3}$$

where H_{cc} is the physical width of the pore, which is defined as the distance from the plane passing through all carbon atoms of the outermost layer of one wall to the corresponding plane of the opposite wall (see Figure 1 overleaf). This formula was first suggested by Everett and Powl (1976), and later by Kaneko *et al*. (1994).

In this way, the adsorption excess (and therefore the adsorption isotherm), as well as other thermodynamic quantities of interest such as the isosteric enthalpy of adsorption, may be calculated.

4. CALCULATING THE PORE-SIZE DISTRIBUTION

Davies *et al*. (1999) and Davies and Seaton (1999, 2000) have addressed the problem of calculating PSDs from adsorption data in detail. We therefore present here only the most important aspects of the solution procedure.

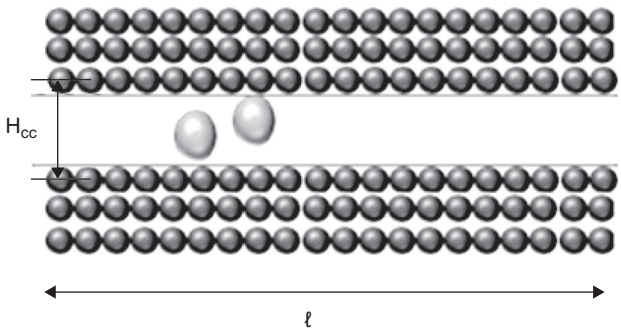

Figure 1. The simulation cell.

The theoretical overall adsorption isotherm (θ^{theor}) can be expressed as a superposition of isotherms corresponding to each pore size (H_j), pressure P and temperature T, called local isotherms, θ_L, each with a weight corresponding to the pore-size distribution, $f(H_j)$:

$$\theta_i^{theor} = \sum_{j=1}^{m} \theta_L(H_j^*, P_i, T)\, f(H_j^*)\, \delta H_j^* \tag{4}$$

where m is the number of quadrature intervals used in the analysis, and H^* is the mid-point of each quadrature interval. Equation (4) cannot be solved directly due to the ill-posed and ill-conditioned properties of these equations. The detrimental effect of both of these properties can, however, be minimized by employing regularization. The PSD is then obtained by fitting equation (4) plus the regularization term numerically, as proposed by Davies and co-workers (Davies *et al*. 1999; Davies and Seaton 1998), via a fast non-negative least-square algorithm. This is the most commonly used method to stabilize the result, incorporating additional constraints that are based on the smoothness of the PSD (Wilson 1992; Szombathely *et al*. 1992; Merz 1980; Whaba 1977; Hansen 1992). Physically, this corresponds to recognizing that a real PSD is more likely to be relatively smooth and centred around a few dominant pore sizes, rather than being highly fragmented and spiky. One complicating factor in employing regularization is that it requires the identification of an optimal smoothing parameter to be used in the analysis. To overcome this difficulty, we have used L curves (Jagiello and Thommes 2004) to determine the optimal amount of smoothing. Such L curves are a plot of some measure of the error of fit to the data against the smoothing parameter. In general, the error of fit to the data increases as the value of the smoothing parameter increases. However, below a threshold value of the smoothing parameter the increase in the error is often negligible, whilst above the threshold the error increases rapidly. Plots of the error against the smoothing parameter therefore resemble an "L" lying on its side. These curves are used to identify this threshold value which is taken to be the optimal extent of smoothing.

PSD solutions satisfying minimum L-curve and generalized cross-validation criteria have been shown to have a superior predictive performance relative to other possible PSD solutions (Davies *et al*. 1999; Davies and Seaton 1999; Pinto da Costa *et al*. 2011).

It is interesting that two PSDs, though different in shape, can give similar predictions that are in good agreement with the "experimental" isotherms. This suggests that several "good" PSDs — in terms of their predictive ability — can exist which represent the porous structure of a carbon (though of course the real material has a unique PSD) (Cai *et al*. 2007).

Pore-size distributions for slit pores have been calculated with kernels containing 37 pore sizes between 4 Å and 40 Å (with a step of 1 Å) and 37 relative pressure points ($2.0 \times 10^{-6} - 0.999$) for N_2, and 12 pore sizes between 4.13 Å and 11.25 Å for CO_2 and 28 relative pressure points ($1.44 \times 10^{-3} - 2.09 \times 10^{-2}$). Gusev and O'Brien (1997) recognized that, for a given set of data, there is a maximum pore size that can be identified reliably in a PSD analysis. Differentiating large pores from one another is difficult because the extent of adsorption is virtually indistinguishable from one pore to another. This arises when the adsorption onto the opposite walls of a single pore occurs essentially independently, i.e. the pore walls become too far away from each other to enhance adsorption. The pore size above which this occurs depends on the adsorptive and is a function of the temperature and the pressure. Gusev and O'Brien (1997) therefore introduced the concept of a "window of reliability" into PSD analyses. This "window" extends from the smallest pore that the adsorptive can enter to the largest pore that can be reliably distinguished from the next largest pore. Since the adsorption in all the pores larger than those in the window of reliability is essentially indistinguishable, assigning a single quadrature interval to this region makes best use of the experimental data (Davies *et al*. 1999).

5. RESULTS AND DISCUSSION

Figure 2 presents a comparison between the experimental isotherms and those obtained by Monte Carlo simulation for N_2 and CO_2 at 77 K and 273 K, respectively. The simulated isotherms show very good agreement with experimental data in all cases. On the other hand, the fact that the adsorption isotherms are clearly of Type I implies that the conditions of impregnation, pressing and carbonization employed in the preparation of the disc-shaped monoliths was adequate to produce microporous solids.

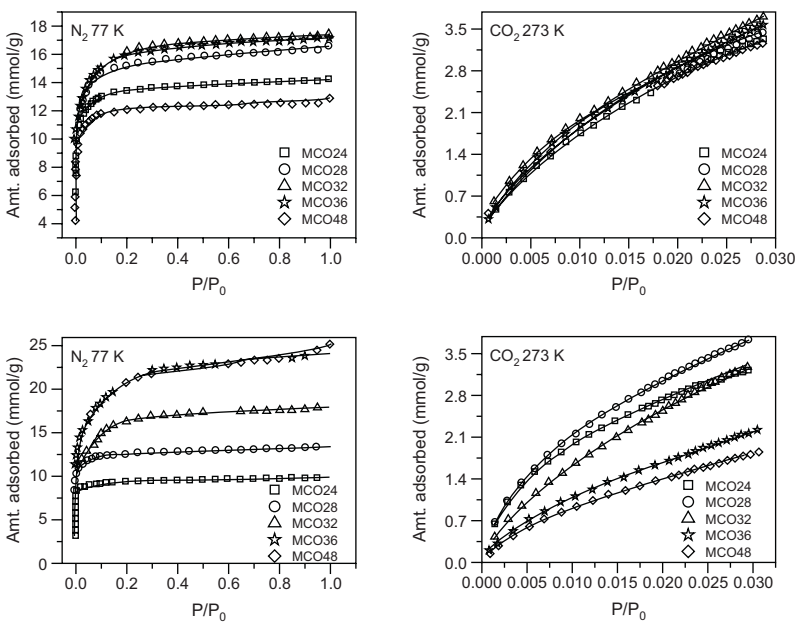

Figure 2. Experimental (symbol) and fitted (line) isotherms for N_2 at 77 K and CO_2 at 273 K.

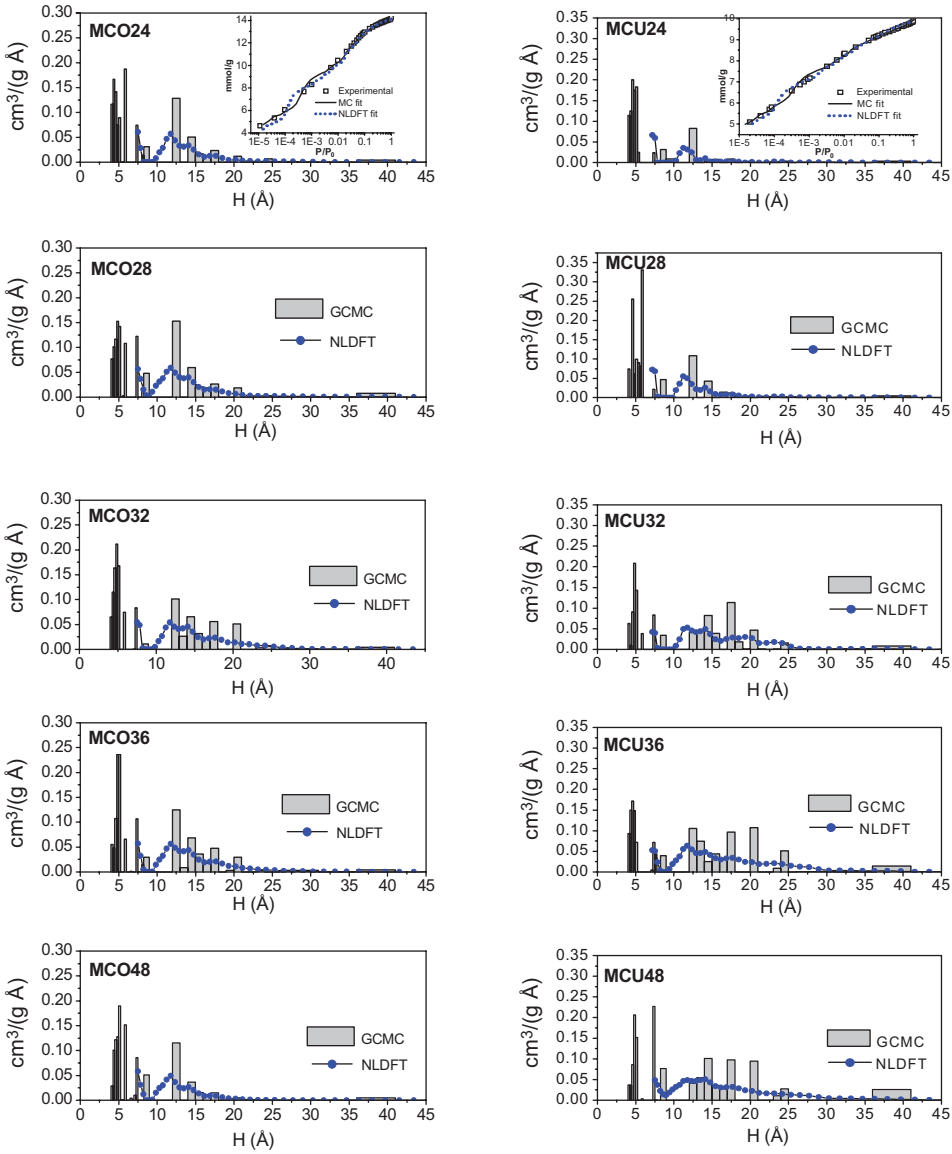

Figure 3. PSDs calculated from the nitrogen isotherms shown in Figure 2 applying the NLDFT (Quantachrome Soft) and the GCMC. The respective insets show the NLDFT and GCMC fits for the MCO24 and MCU24 samples.

Figures 3 and 4 show the PSDs predicted by the adsorption of N_2 and CO_2 for all samples. In these PSDs, it is clear that the activation treatment performed, based on the impregnation of precursors with H_3PO_4 solutions, led to the development of porosity in two regions, i.e. in the ultramicropore region and in the high-micropore and near-mesopore region. In the case of nitrogen adsorption onto MCU samples, there is a special increase in the porosity in the latter region when the concentration of active agent is increased. Furthermore, from Figure 3, it can be

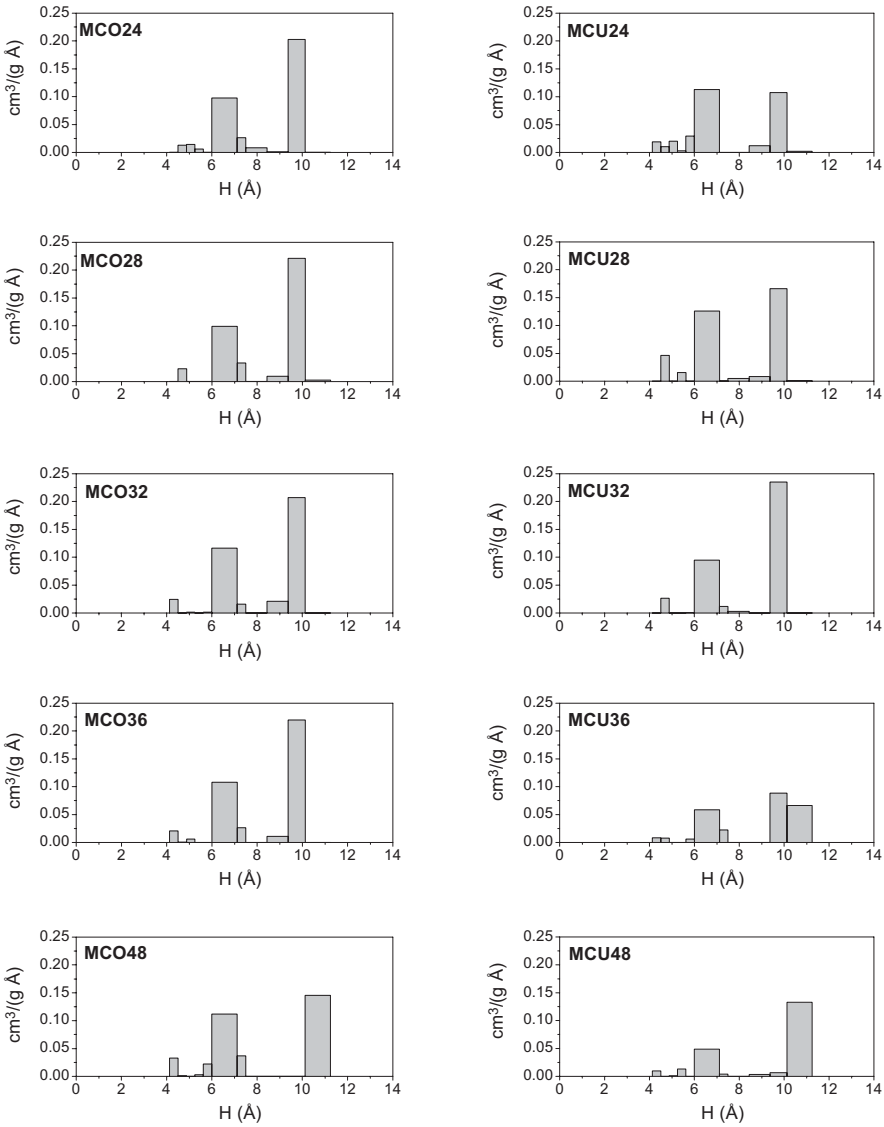

Figure 4. PSDs of activated carbon monoliths obtained by GCMC simulation for CO_2 at 273 K.

seen that the PSDs calculated from the nitrogen isotherms applying the Non-Local Density Functional Theory (NLDFT) (Quantachrome Soft) showed good agreement with the MS-PSDs.

The PSDs predicted by the adsorption of N_2 and CO_2 in the ultramicropore region were in good agreement for all the samples (considering that the N_2 PSD was biased due to the 1 nm pore-size gap due to the absence of heterogeneity), a behaviour that is not always observed (Débora *et al*. 2010, 2011; de Oliveira *et al*. 2011; Toso *et al*. 2010).

From the PSDs predicted by the simulation analysis, other textural parameters such as the surface area and the micropore volume can be obtained and their values compared with those

TABLE 2. Textural Characteristics of the Discs: Micropore Volume, W_0, Surface Area and Immersion Enthalpy

Sample	Nitrogen adsorption		CO_2 adsorption		Nitrogen adsorption		ΔH_{inm} benzene (J/g)
	DR	MC	DR	MC	BET	MC	
	$W_{0\ total}$ (cm^3/g)	$W_{0\ total}$ (cm^3/g)	$W_{0\ ultramicr}$ (cm^3/g)	$W_{0\ ultramicr}$ (cm^3/g)	Surface area (m^2/g)	Surface area (m^2/g)	
MCO24	0.40	0.51	0.22	0.29	1125	1289	120.2
MCO28	0.46	0.59	0.23	0.31	1270	1354	130.0
MCO32	0.44	0.62	0.24	0.32	1320	1404	147.7
MCO36	0.45	0.61	0.23	0.32	1318	1386	132.3
MCO48	0.36	0.47	0.20	0.33	975	1190	112.9
MCU24	0.32	0.37	0.19	0.25	752	1148	96.02
MCU28	0.42	0.49	0.21	0.30	1013	1340	123.3
MCU32	0.45	0.63	0.21	0.30	1397	1217	130.1
MCU36	0.59	0.83	0.14	0.22	1711	1555	119.5
MCU48	0.61	0.86	0.11	0.22	1706	1497	111.9

predicted by the BET and DR equations. Table 2 presents such a comparison for the different samples studied. It is well known that the BET equation always provides an over-estimation of the surface area for micropores, while the DR equation provides a realistic estimation of the total micropore volume. The series of ACMs prepared from coconut shells presented BET surface areas between 975 m^2/g and 1320 m^2/g, micropore volumes between 0.36 cm^3/g and 0.45 cm^3/g, ultramicropore volumes between 0.21 cm^3/g and 0.24 cm^3/g, and a maximum adsorbed volume of nitrogen of 520 cm^3/g. The monoliths synthesized from African palm pits presented an adsorbed nitrogen volume of 450 cm^3/g, BET surface areas between 752 m^2/g and 1711 m^2/g, micropore volumes between 0.30 cm^3/g and 0.60 cm^3/g, and ultramicropore volumes between 0.19 cm^3/g and 0.21 cm^3/g.

From Table 2, it can be observed that the MC predictions for the surface area seemed to be more consistent than the BET predictions. In fact:

1. For the MCO series of ACMs, the MC surface area attained a maximum value for a concentration value of the activation agent equal to 32 w/v% and then decayed slightly for higher values, accompanied by a decrease in the total micropore volume, while the ultramicropore volume was almost constant. In contrast, the BET surface area experiments showed a strong decrease when the activation agent concentration was greater than 32 w/v%. Hence, the behaviour of the surface area was more consistent with that of the micropore volume for MC simulations.
2. For the MCU series of ACMs, the MC surface area again showed a maximum for a concentration value of the activation agent equal to 32 w/v% and then decayed, while the BET surface area showed a steady increase. On the other hand, the total micropore volume increased steadily while the ultramicropore volume showed a notable decrease for high concentrations of the activation agent, which should produce a decrease in the BET surface area. Hence, the behaviour of the BET surface area was again more consistent with that of the micropore volume for MC simulations.

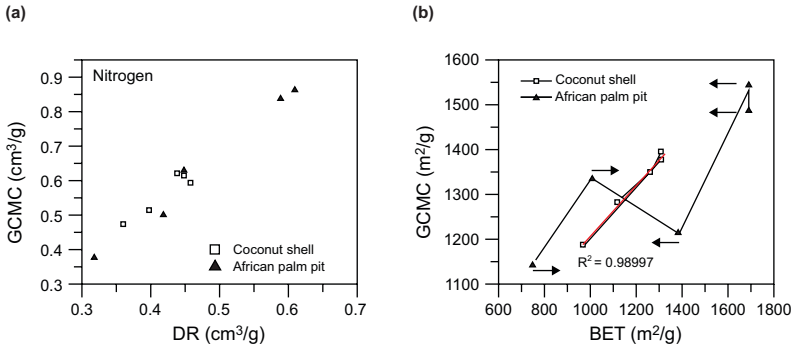

Figure 5. Relationship between DR and BET textural parameters and those obtained by GCMC simulation for the ACMs: (a) micropore volume; (b) surface area.

Figure 5 shows the correlation between the DR values for the micropore volumes and the BET values for the surface areas together with the corresponding values predicted by MC simulation, thereby aiding visualization of the above discussion. The behaviour of the total micropore volumes in Figure 5(a) shows a good correlation between the DR values and the simulated data for the two series. When making a comparison between the surface areas determined by BET and MC methods, it is important to remember that the BET model usually over-estimates the surface area of microporous solids. This is because it computes the areas of all the nitrogen molecules that fill the pores, regardless of whether they are in touch with the pore surface or not. However, for very small pores, viz. less than two molecular diameters, the BET values under-estimate the surface area. For the surface areas depicted in Figure 5(b), the trend for the MCO samples was satisfactory. Thus, as shown in Table 2, the BET areas in all the samples of this series, although lower than those predicted by Monte Carlo simulation, did deviate significantly from each other. This can be explained from the PSDs presented in Figure 3, where there is a balance between the narrow pore volumes (ca. 5 Å) and pore volumes for larger sizes. On the other hand, the MCU samples did not show a definite trend. Again, as in the previous case, the PSDs can explain this behaviour. Thus, samples MCU24 and MCU28 contained a large volume of pores of approximately 5 Å size, in which there was not enough space to accommodate two layers of nitrogen molecules each of 3.6 Å size, thereby producing an under-estimation of the surface area. In addition, the pore volume for larger sizes was not sufficient to compensate for this phenomenon, thus resulting in an overall under-estimation of the surface area. In contrast, in the other samples in this series, the PSDs showed a higher proportion of pores larger than 10 Å, in which more than two parallel nitrogen molecules layers could be accommodated, thereby causing an over-estimation of the surface area, as evidenced by the data listed in Table 2. Taking this into account, if the values of the BET area can be shifted hypothetically, in an appropriate way, as indicated in the figure by the arrows for each sample, there would be a good correlation between the areas determined by BET and MC.

Figure 6 overleaf shows the relationship between the enthalpies of immersion into benzene, as determined experimentally, and the surface areas, as obtained via the BET equation and MC simulations. According to previous work, the enthalpy of immersion in benzene should increase with the surface area (Moreno and Giraldo 2000). This regular trend is observed for the MCO samples in Figure 6(a), where the enthalpy value increased with increasing BET area in an almost linear fashion, with the exception of sample MCO32 which presented a high value for the enthalpy of immersion in benzene (147 J/g), but a surface area value very similar to the MCO36 monolith. The PSD for MCO32

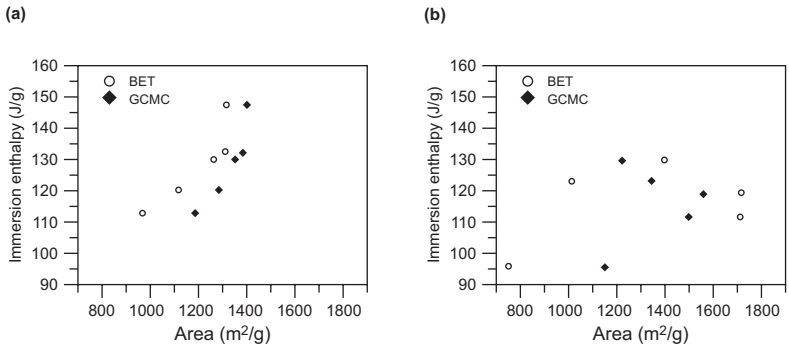

Figure 6. Relationship between the immersion enthalpy and the areas obtained by BET and GCMC for (a) coconut shell and (b) African palm pit.

shows that this sample contained a greater volume of pores of ca. 20 Å diameter compared with others in the series, thereby explaining its high enthalpy of immersion in benzene as a result of the interaction of a larger number of benzene molecules with the solid. However, in the case of samples taken from African palm pit, Figure 6(b) shows an initial increase in enthalpy with the surface area up to sample MCU32, but thereafter a decrease for those samples with higher BET area values corresponding to higher concentrations of phosphoric acid. As can be seen from the PSDs for these samples, a partial collapse/shrinkage of the porous structure occurred for those samples prepared using high concentrations of H_3PO_4 as the impregnating agent. Phosphoric acid can produce metaphosphates which can block some of the porous structure of the sample, preventing its interaction with the benzene molecule and thus producing a decrease in the heat of immersion. Apparently, this effect is more sensitive for a larger molecule such as benzene. Most probably, in these samples, the swelling of the porous structure modifies the pore size and shape in such a way that the nitrogen molecule is capable of accessing the porosity while the benzene molecule experiences kinetic restrictions.

5. CONCLUSIONS

We have compared the textural characteristics and energy parameters of activated carbon monoliths prepared from coconut shell and African palm pit, through an analysis of adsorption and calorimetric data carried out using Monte Carlo simulation methods.

Samples of disc-type activated carbon monoliths obtained from coconut shells had a micropore volume in the range 0.36–0.45 cm^3/g, BET area values in the range 975–1320 m^2/g, and micropore and mesopore distributions appropriate to achieve efficient adsorption. The best characteristics were obtained for the MCO36 and MCO32 series.

With respect to the disc-type monoliths obtained from African palm pit, these had a micropore volume in the range 0.32–0.61 cm^3/g, BET area values in the range 752–1711 m^2/g, and micropore and mesopore distributions again appropriate to achieve efficient adsorption. The best characteristics were obtained for the MCU48 and MCU36 series.

We stress the importance of using a method based on first principles, independent of the adsorption mechanism — such as Grand Canonical Monte Carlo simulations — to analyze the data through the calculation of the PSD for the material. Such an approach should provide the most complete information available for the correct characterization of the adsorption properties of the material.

ACKNOWLEDGMENTS

The authors wish to thank the Master Agreement established between the University of the Andes and the National University of Colombia and the Memorandum of Understanding entered into by the Departments of Chemistry of both universities. CONICET is also gratefully acknowledged for financial support for this research.

REFERENCES

Allen, M.P. and Tildesley, D.J. (1987) *Computer Simulation of Liquids*, Clarendon Press, Oxford, U.K.
Almansa, C., Molina-Sabio, M. and Rodríguez-Reinoso, F. (2004) *Microporous Mesoporous Mater.* **76,** 185.
Azevedo, D.C.S., Rios, R.B., López, R.H., Torres, A.E.B., Cavalcante, C.L., Toso, J.P. and Zgrablich, G. (2010) *Appl. Surf. Sci*. **256,** 5191.
Bansal, R.C. and Goyal, M. (2005) *Activated Carbon Adsorption*, Taylor & Francis, London, U.K.
Budinova, T., Ekinci, E., Yardim, F., Grima, A., Bjornobom, E., Minkova, V. and Goranova, M. (2006) *Fuel Process Technol*. **87,** 899.
Cai, Q., Buts, A., Biggs, M.J. and Seaton, N.A. (2007) *Langmuir* **23,** 8430.
Cao, D. and Wu, J. (2005) *Carbon* **43,** 1364.
Davies, G.M. and Seaton, N.A. (1998) *Carbon* **36,** 1473.
Davies, G.M. and Seaton, N.A. (1999) *Langmuir* **15,** 6263.
Davies, G.M. and Seaton, N.A. (2000) *AIChE J*. **46,** 1753.
Davies, G.M., Seaton, N.A. and Vassiliadis, V.S. (1999) *Langmuir* **15,** 8235.
de Oliveira, J.C.A., López, R.H., Toso, J.P., Sebastião, M.P., Cavalcante, C.L. and Zgrablich, G. (2011) *Adsorption*, DOI 10.1007/s10450-011-9343-5.
Débora, A., Soares, M., de Oliveira, J.C.A., Toso, J.P., Sapag, K., López, R.H., Azevedo, D.C.S., Cavalcante, C.L. and Zgrablich, G. (2011) *Adsorption,* DOI 10.1007/s10450-011-9344-4.
Débora, A., Soares, M., Toso, J.P., Sapag, K., López, R.H., Azevedo, D.C.S., Cavalcante, C.L. and Zgrablich, G. (2010) *Microporous Mesoporous Mater*. **134,** 181.
Everett, D. and Powl, J.J. (1976) *J. Chem. Soc., Faraday Trans*. **72,** 619.
Frenkel, D. and Smit, B. (1996) *Understanding Molecular Simulation*, Academic Press, Amsterdam, The Netherlands.
Gusev, V.Y. and O'Brien, J. (1997) *Langmuir* **13,** 2815.
Hansen, P.C. (1992) *SIAM Rev*. **24,** 561.
Jagiello, J. and Thommes, M. (2004) *Carbon* **42,** 1225.
James, B.C. (Ed) (2006) *Surface Area and Porosity Determination by Physisorption*, Elsevier, Oxford, U.K., pp. 29–53.
Kaneko, K., Cracknell, R. and Nicholson, D. (1994) *Langmuir* **10,** 4606.
Konstantakou, M., Steriotis, Th.A., Papadopoulos, G.K., Kainourgiakis, M., Kikkinides, E.S. and Stubos, A.K. (2007) *Appl. Surf. Sci.* **253,** 5715.
Liu, L., Liu, Z., Huang, Z., Liu, Z. and Liu, P. (2006) *Carbon* **44,** 1598.
Merz, P.H. (1980) *J. Comput. Phys*. **38,** 64.
Moreno, J.C. and Giraldo, L. (2000) *Instrum. Sci. Technol*. **28,** 171.
Nakagawa, Y., Molina-Sabio, M. and Rodriguez-Reinoso, F. (2007) *Microporous Mesoporous Mater.* **103,** 29.
Nicholson, D. and Parsonage, N.G. (1982) *Computer Simulation and the Statistical Mechanics of Adsorption*, Academic Press, London, U.K.
Pinto da Costa, J.M.C., Cracknell, R.F., Seaton, N.A. and Sarkisov, L. (2011) *Carbon* **49,** 445.
Ravikovitch, P.I., Vishnyakov, A., Russo, R. and Neimark, A.V. (2000) *Langmuir* **16,** 2311.
Rodríguez-Reinoso, F. and Molina-Sabio, M. (1998) *Adv Colloid Interface Sci*. **76/77,** 271.

Rodríguez-Reinoso, F., Almansa, C. and Molina-Sabio, M. (2003) *Spanish Patent 2165784* (Universidad de Alicante).
Silvestre-Albero, J., Gómez, C., Sepúlveda-Escribano, A. and Rodríguez-Reinoso, F. (2001) *Colloid Surf. A* **187,** 151.
Sing, K.S.W. (1989) *Colloids Surf.* **38,** 113.
Sing, K.S.W. (2004) *Colloids Surf. A* **241,** 3.
Steele, W.A. (1974) *The Interaction of Gases with Solid Surfaces*, Pergamon Press, Oxford, U.K.
Szombathely, M.V., Brauer, P. and Jaroniec, M. (1992) *J. Comput Chem.* **13,** 17.
Toso, J.P., López, R.H., Azevedo, D.C.S., Cavalcante, C.L., Prauchner, M.J., Rodríguez-Reinoso, F. and Zgrablich, G. (2010) *Adsorption,* accepted for publication.
Valladares, D.L., Rodríguez-Reinoso, F. and Zgrablich, G. (1998) *Carbon* **36,** 1491.
Vishnyakov, A. and Neimark, A.V. (2003) *Langmuir* **19,** 3240.
Whaba, G. (1977) *SIAM J. Numer. Anal.* **14,** 651.
Wilson, J.D. (1992) *J. Mater Sci.* **27,** 3911.
Yates, M., Blanco, J., Avila, P. and Martin, M.P. (2000) *Microporous Mesoporous Mater*. **37,** 201.